



Detection of changes in the heat emissions signature of buildings related to indoor activity using publicly available satellite data

Mario E. Suaza-Medina¹ · Javier Lacasta¹ · Francisco J. López-Pellicer¹ · Béjar Rubén¹ · F. Javier Zarazaga-Soria¹

Received: 1 October 2024 / Accepted: 16 May 2025
© The Author(s) 2025

Abstract

Monitoring human activities in remote areas presents significant challenges due to lacking communication networks and infrastructure. In this context, using publicly available satellite imagery offers a cost-effective solution, as it enables the identification of changes in these areas. However, specific scenarios make detection more complicated. One such scenario is detecting indoor activity within buildings in remote areas. Walls and roofs create barriers for most sensors. Nevertheless, activities inside buildings can be associated with heat emissions, which specific remote sensors can detect. Unfortunately, publicly available satellite data does not include information from such sensors. In light of this limitation, this study investigates the opportunity of using machine learning models to interpret public-available data. Specifically, we trained four machine learning models (XGBoost, LGBM, DNN, and CNN) using images from Sentinel-2 Band 12 (the sensor with the frequency range closest to the heat emission peak) and meteorological data (temperature). Our results show that these models can identify farm-building activity, with the XGBoost model achieving the highest accuracy of 0.96 by integrating satellite data and temperature information; the findings suggest that leveraging public satellite sensors can effectively detect human heat emissions and improve surveillance in remote areas, overcoming some limitations of traditional methods.

Keywords Machine learning · Neural networks · Satellite image · Remote sensing

Introduction

Human activities in remote areas are often challenging to monitor and control due to the lack of infrastructure and communication networks. For instance, a hut far from roads and communication networks can be easily used without authorisation (even for illegal business). In this context, using

publicly available satellite imagery offers a cost-effective solution, as it enables the identification of changes in these areas. However, there are many scenarios where detection becomes more complex.

One such scenario involves detecting indoor activity within buildings in remote areas. Human indoor activities in this context include any that can be associated with variations in the temperature inside a building, which may be linked to heat emissions from the building. These activities might include using heaters, cooling systems, high-temperature machinery, and agricultural operations such as livestock housing or crop drying. Also, industrial processes like metalworking, food processing, and storage of temperature-sensitive materials can contribute to detectable heat variations. The range of emissions (8000–14000 nm) is important for such detections, and the challenge lies not in the absence of sensors capable of detecting these wavelengths but in the lack of sensors with sufficient resolution in this range. Walls and roofs often obstruct sensors, and the available resolution limits the ability to pinpoint variations effectively; this limitation complicates the detection of routine and potentially illicit activities, such as unauthorized occupancy, drug

Communicated by: Hassan Babaie

✉ Mario E. Suaza-Medina
mesuaza@unizar.es

Javier Lacasta
jlacasta@unizar.es

Francisco J. López-Pellicer
fjlopez@unizar.es

Béjar Rubén
rbejar@unizar.es

F. Javier Zarazaga-Soria
javz@unizar.es

¹ Aragon Institute of Engineering Research (I3A), Universidad de Zaragoza, C. María de Luna, Zaragoza 50018, Aragón, Spain

Table 1 Sentinel-2 resolution and spectral bands

Spatial Resolution Resolution (Meters/Pixel)	Band	Wavelength (nm) ^c	Spectral Resolution			
			Central Wavelength (S2A) ^a	Bandwidth (S2A)	Central Wavelength (S2B) ^b	Bandwidth (S2B)
10	B2	490	492.7	65	492.3	65
	B3	560	559.8	35	558.9	35
	B4	665	664.6	30	664.9	31
	B8	842	832.8	105	832.9	104
20	B5	705	704.1	14	703.8	15
	B6	740	740.5	14	739.1	13
	B7	783	782.8	19	779.7	19
	B8a	865	864.7	21	864	21
	B11	1610	1613	90	1610.4	94
60	B12	2190	2202.4	174	2185.7	184
	B1	443	442.7	20	442.2	20
	B9	940	945.1	19	943.2	20
	B10	1375	1373.5	29	1376.9	29

^a **S2A**: Refers to the first satellite of the Sentinel-2 mission.

^b **S2B**: Refers to the second satellite of the Sentinel-2 mission, complementing S2A for higher temporal resolution.

^c **nm**: Nanometers, a unit of measurement for wavelengths in the electromagnetic spectrum

production, human trafficking, illegal migration, or similar activities (Sarrica 2022; Tellman et al. 2020; Avila-Zuniga-Nordfjeld et al. 2023; Froehlich and Taiatu 2020).

In light of this limitation, this study investigates the feasibility of using machine learning models to interpret the current public-available data. Specifically, we analyse if detecting the wavelengths of activity emissions outside the emission peak that overlap with the satellite sensors range is possible. We have focused on the Copernicus Sentinel-2 mission¹, which provides frequent data updates and detects a broad range of frequencies. It consists of two polar-orbiting satellites placed in the same sun-synchronous orbit with a revisit time between 2 and 5 days, depending on the latitude and under cloud-free conditions. Each satellite has sensors for the twelve bands shown in Table 1. Among these, the B12 band is the closest to human heat emissions, operating at a central wavelength of 2202.4 nm for sensor S2A and 2185.7 nm for S2B (The-European-Space-Agency 2015) and is used to identify snow, ice, and clouds (water absorption emission). This band operates in the near-infrared spectrum rather than the thermal infrared range (8000–14000 nm) typically associated with human heat emissions. In this study, "heat signals" refer to patterns in the spectral response of the B12 band that indirectly indicate variations in building conditions, such as human activities or equipment usage, inferred through machine learning models.

Since the sensor data cannot be directly interpreted as heat signals, we have trained different neuronal network models to learn to interpret it. Specifically, we have compared the performance of Dense Neural Networks (DNN), Convolutional Neural Network (CNN), Extreme Gradient Boosting (XGBoost) and Light Gradient Boosting Machine (LGBM) models due to their suitability and accuracy in similar contexts (Bal and Kayaalp 2021; Tos et al. 2021). These models have been trained with images of a selection of buildings obtained from the Sentinel-2 B12 sensors taken at different moments, information about the state of use of the building in each image, and meteorological data with the daily temperature in each area used for training. The models infer activity patterns that correlate with variations in the spectral response of the B12 band. As a summary of the above, the most innovative aspects that could be considered as contributions of this work are:

- **Innovative use of the B12 band (SWIR, ~2200 nm)**: Utilized to indirectly detect human activity, beyond its conventional application in snow, moisture, and cloud detection.
- **Off-peak thermal emission detection (outside 8000–14000 nm)**: Explores alternative wavelengths where traditional thermal sensors do not operate, enabling new possibilities in remote sensing.
- **Focus on remote sites and isolated buildings**: Targets infrastructure in rural, clandestine, or distant areas—contexts rarely addressed in current literature.

¹ <https://sentinels.copernicus.eu/web/sentinel/missions/sentinel-2>, Last visit October 2024

- **Alternative to traditional thermal sensors:** Addresses challenges like low spatial resolution, persistent cloud cover, or low temporal frequency of thermal satellites.
- **None of the reviewed works detect human presence in remote facilities using B12 or SWIR, and existing studies focus on environmental or agricultural variables:** No prior studies explore this possibility explicitly, as most works apply Sentinel-2 to parameters like geology, salinity, crop growth, or biomass-not to activity-based detection.
- **Unprecedented combination: off-peak thermal detection + ML + remote surveillance:** No reviewed research addresses the joint use of these three components with Sentinel-2 B12.

The rest of the paper is structured as follows. The following section presents a state-of-the-art revision related to the proposed hypothesis. Section “[Materials and methods](#)” describes the experiment designed. After this, the results of the investigation are discussed. The paper ends with a conclusion and future applications and studies based on the results of the experiment.

Related work

Recent technologies and advances in satellite imagery have encouraged data classification initiatives using machine learning techniques in multiple areas, such as agriculture, environment, cartography, topography, and urban planning.

In the agriculture and environment field, Zhou et al. (2018) implemented a CNN and SVM to classify different crop types in satellite images; these techniques are more precise and efficient crop management by distinguishing types such as rice, peanuts, and corn. The research by Yan et al. (2021) proposed a method based on discrete grids with machine learning to integrate GaoFen-1 and Sentinel-2 imagery for large-scale crop mapping. In Vasilakos et al. (2020), the researchers took advantage of the high spectral and spatial resolution sensors of sentinel-2 to monitor changes in the Mediterranean ecosystem. They tested six traditional classifiers and nine ensemble classifiers based on voting methods. Similarly, Alshari and Gawali (2020) used Sentinel-2 images to identify vegetation cover and land use with different strategies based on the analysis of pixels, objects, rules, distance, and the use of neural networks. Concurrently, Kim et al. (2022) utilised Sentinel-2 multispectral bands to detect chlorophyll in optically complex inland and coastal waters, employing machine-learning regression models. Liu et al. (2022) identified high-risk environments for disease transmission using WorldView-2 satellite photos enhanced with semantic segmentation techniques. In recent studies, Alberto Vavassori and Brovelli (2023) compared the effectiveness of multi-

spectral (Sentinel-2) and hyperspectral (PRISMA) imagery in Local Climate Zone (LCZ) classification. Their research used seasonal imagery, the PRISMA mission, and Sentinel-2 images to capture and analyse vegetation variations. In the study proposed by Zhang et al. (2021), and in the investigations by Abdollahi et al. (2022); Dhedia et al. (2021), the Random Forest algorithm was employed, fine-tuned through Bayesian optimisation for land cover identification using Sentinel-2 imagery. They used a deep learning model (U-Net) in their solution to analyse the images and produce segmentation maps for the aquatic vegetation where the snail tends to have its habitat. Dhedia et al. (2021) studied the characterisation of the terrain of the geographical area using Sentinel-2 images and a Random Forest algorithm. This approach emphasises the importance of accurate terrain mapping in understanding and managing the ecological footprint of various landscapes. Moreover, Ge et al. (2022) proposed a hybrid learning framework that combines Sentinel-2 data (except B1) and environmental covariates to identify problems in soil salinisation. This methodology, employing reinforced gradient regression trees, illustrates the integration of environmental data with multispectral imaging for focused ecological applications. In Suaza-Medina et al. (2024), a predictive model was developed to accurately determine the optimal maize harvest date, ensuring sustainable food production amid growing global demand. This model utilises the Normalised Difference Vegetation Index (NDVI) and climatological data, highlighting the significant impact of atmospheric pressure, mean temperature, precipitation, and NDVI on the prediction outcomes.

Satellite imagery is also broadly used for urban planning, monitoring, and identification of land use. Pati et al. (2020) introduced a hybrid approach combining supervised and unsupervised learning techniques to detect changes in remote sensing images, enhancing the detection accuracy by considering the spatial relationships of adjacent pixels. Dixit et al. (2022) proposed a methodology for extracting buildings in images obtained from Sentinel-2 and OpenStreetMap. They use all Sentinel-2 high-resolution bands, including the SWIR and enhanced multispectral satellite images with information on impervious surfaces. The study by Memduhoğlu et al. (2024) proposed to classify urban building functions by using large language models (LLMs) combined with OpenStreetMap (OSM) labels and spatial and physical data, and this approach highlights how LLMs improve the interpretation of geospatial labels in urban environments, the research shows how this integration can help improve feature classification in different areas of the city. Chen et al. (2022) introduced a novel Res2-Unet framework for detecting buildings in aerial images. This framework innovates using a two-step process involving segmentation and conditional random field (CRF) refinement to enhance building boundary accuracy. Furthermore, Paul and Bhounik (2022)

Suggested the HyperUNet architecture, a novel approach for hyperspectral image classification. This methodology incorporated spectral partitioning techniques, improving variance in pixel values and limited labelled data. Wang and Hu (2022) used machine learning to identify rural architecture for China rural development. They introduced a new Recog-Net model. This model incorporated the histogram of oriented gradients (HOG), used for contour feature extraction and combined with an SVM classifier for feature classification. Wahbi et al. (2023) directed their attention towards detecting and mapping settlements in rural regions of Morocco using deep learning algorithms and Sentinel-2 satellite images. Their study tests the performance of the UNet convolutional neural network architecture and the deep Residual UNet (ResUNet) model. In parallel, Chen et al. (2023) introduced an innovative building extraction method for large-scale satellite imagery. This method utilises super-resolution and instance segmentation with a lower-resolution open dataset and an advanced R-CNN with a Multi-Path Vision Transformer. Meanwhile, Song and Lu (2024) developed a model that combines ResNet and LSTM neural networks to analyse remotely sensed images and temporal data, better capturing the evolution of urban landscapes; this method allows more accurate classification of features within a city, like Nurkarim and Wijayanto (2023) also investigated the use of neural networks to interpret aerial imagery, using both visual and temporal features to classify urban functions. Du et al. (2024) explored urban satellite image segmentation using deep learning techniques, focusing on urban landscape analysis, and Munyati (2024) studied the effect of temperature on urban vegetation using thermal imagery trying to understand how temperature influences vegetation behaviour in cities, thus aiding in urban green space conservation planning.

Regarding land use classification, Talukdar et al. (2020) propose multiple land-use/land-cover (LULC) mapping models. These models cater to the nuanced demands of precise land cover classification, which is critical for effective land management and planning. The investigation by Rahman et al. (2020) centred on the comparative assessment of diverse machine learning algorithms for satellite image classification, focusing explicitly on rural and urban areas. They aimed to identify suitable algorithms for detecting land use and land cover change (LULCC) in fragmented regions. Their work aimed to fine-tune the accuracy of satellite-based classifications, which are essential for monitoring and managing fragmented habitats and landscapes. A separate investigation by Abdollahi et al. (2022) applied a LeNet network for high-resolution grassland mapping based on Sentinel-2, Landsat and stationary time series imagery. The resulting maps were compared with existing systems, such as the Australian Land Use and Management and the Dynamic Land Cover Dataset. Khurana et al. (2023) used multi-temporal Sentinel-2 imagery to classify land cover in urbanised areas,

employing support vector machines (SVMs) and testing different algorithms to improve accuracy. Sirous et al. (2023) developed a generative adversarial network to classify urban land uses using data from different sources, thus improving the classification accuracy.

The thermal detection context studied in this paper has a prominent area of focus. An illustrative example is the work of Cho et al (2018). Utilising the Shortwave Infrared (SWIR) band from Landsat-8, they developed a refined algorithm for disaggregating Thermal infrared (TIR) images. Following this line of research, Marchese et al. (2019) applied satellite imagery from Sentinel-2 and Landsat-8 to map volcanic thermal anomalies on a global scale. They integrated TIR and SWIR sensor data to identify volcanic hot pixels in daylight. In the study by Kato et al. (2021), they use Convolutional Neural Networks (CNNs) combined with decision trees to effectively classify high-temperature heat sources from Landsat and Sentinel-2 images. dos Santos (2020) produced a parsimonious model to retrieve maximum air temperature (Tmax) at high spatiotemporal resolution using Earth Observation (EO) satellite data for London over eleven years; they employed six different machine learning algorithms to estimate Tmax within an urban context. Garzón et al. (2021) developed models using a combination of Sentinel-2 and Landsat imagery to study heat islands in urban areas, and Liu et al. (2021) studied how factory characteristics such as scale and structure impact local temperatures, providing insights to improve environmental management practices. Another example is in Hrisko et al. (2021), which utilised a gradient-boosted regression model alongside a hysteresis model derived from satellite data to estimate urban heat storage. Kafy et al. (2021) examined the effects of rapid urbanisation on changes in land use/land cover (LULC) and land surface temperature (LST); the research provided detailed insights into pattern recognition and temperature fluctuations resulting from urban sprawl. In addition, Lyu et al. (2022) proposed a cyberGIS framework that integrates multiple machine learning models to predict Urban Heat Island effects with fine spatiotemporal granularity. Finally, Natale et al. (2023) introduced Physically Consistent Neural Networks (PCNNs), which were extended to multi-zone building thermal models. These networks maintain physical compliance and capture unknown nonlinear dynamics. Their study's results demonstrated significant accuracy improvements over linear and residual models.

Recent Research in supplemental thermal radiation detection using satellite data has advanced due to its accessibility, high spatial and temporal resolution, and suitable spectral capability. Recent studies have explored the indirect use of the Sentinel-2 B12 band for thermal monitoring, highlighting its utility in soil type discrimination, mineral identification, and soil moisture analysis (Thomas et al., 2022). Specifically, spectral combinations that include the B12 band have

proven effective for discriminating minerals with differentiated thermal properties, thus facilitating the indirect detection of thermal anomalies on terrestrial surfaces (Anifadi et al., 2024). However, despite these advancements, there is a gap in the current scientific literature regarding the specific utilization of Sentinel-2's B12 band for indirect or direct thermal detection, especially concerning precise estimation of supplemental thermal radiation in complex environmental scenarios such as remote sites, isolated buildings, and areas distant from urban settings. Although novel approaches combining multispectral images with advanced machine learning techniques for mapping properties like aboveground biomass and soil salinity exist (Sirpa-Poma et al., 2023; Wang et al., 2024), these studies have not adequately delved into the specific exploitation of the B12 band for indirect thermal inference in remote and isolated environments. This gap highlights the need to expand Research in this area, evaluating this band's capability and practical limitations for indirect or direct thermal applications. Furthermore, current methodologies focus on direct thermal sensing using infrared bands from specialized satellites like Landsat and MODIS; although widely validated, these methods encounter resolution and temporal frequency limitations. Recent studies suggest that indirect detection methods using Sentinel-2's with higher spatial and temporal resolution could significantly overcome these constraints, particularly by exploiting shortwave infrared bands such as B12, which can indirectly indicate temperature variations through spectral response changes linked to surface moisture and vegetation stress (Heath et al., 2024). Moreover, using Sentinel-2 B12 for indirect thermal monitoring is advantageous and novel in monitoring isolated and remote buildings or facilities. This application has been preliminarily explored with promising results, showing significant correlations between B12 reflectance values and indicators of human activity or structural integrity changes in isolated areas (Comparetti and Marques da Silva, 2022).

Algorithms such as Random Forest (RF) and Support Vector Machines (SVM) have demonstrated efficacy in related applications (Anifadi et al., 2024; Sirpa-Poma et al., 2023); this study aims to contribute new results that enhance precision in identifying and monitoring supplemental thermal radiation. New advancements in deep learning techniques can offer new pathways to enhance the usability of Sentinel-2 data. These techniques have successfully improved spatial resolutions, allowing even finer indirect thermal phenomena detection in remote and sparsely populated areas. This enables more precise analyses of subtle temperature-related changes indicative of human or natural activities in remote locations (Lac et al., 2023). Despite these developments, significant methodological challenges remain. Most notably, the calibration of Sentinel-2 data for thermal inference requires extensive and expensive ground truthing, which is limited

by logistical and financial constraints. Integrating Sentinel-2 data, especially the B12 band, with computational methods and field validation improves environmental monitoring and remote site surveillance; this research approach addresses current methodological gaps and can expand the scope of applications for Sentinel-2's indirect thermal sensing capabilities, which can facilitate managing remote and isolated environments and for instance, improving the detection and monitoring of unauthorized activities, isolated industrial operations, and environmental disturbances in remote areas through enhanced thermal detection methods. Thus underpinning the broader significance of advancing this research domain.

Previous studies have demonstrated using multispectral and thermal imagery for vegetation analysis, land use classification, and urban planning. However, it faces limitations in detecting remote area occupancies based on heat emissions. Thermal infrared (TIR) bands often lack the spatial resolution required for detailed occupancy assessments and are not always available in publicly accessible datasets. Multispectral bands like SWIR (Shortwave Infrared) remain underutilised for such purposes despite their ability to penetrate environmental obstructions such as haze, smoke, and thin clouds. This study leverages the Sentinel-2 SWIR band (Band 12) and machine learning techniques, improving the accuracy of detecting human activity under challenging environmental conditions, providing a robust solution for:

- **Governmental Monitoring and Control:** This methodology facilitates governmental bodies' monitoring of agricultural facilities, enabling enhanced oversight in subsidies, taxation, and product traceability. By providing accurate occupancy data, authorities can cross-verify farmer declarations and ensure compliance with regulations. This capability is especially relevant in regions like the Ebro Valley, where agricultural activities play a crucial role in the economy and require effective monitoring to ensure compliance and support governmental planning efforts.
- **Detection of unauthorized use:** This approach identifies unauthorised building usage in remote or sparsely monitored areas. This capability is valuable for detecting illicit activities or ensuring facilities comply with their declared purpose.
- **Animal rescue and disaster preparedness:** While not directly prioritizing rescue efforts, this methodology can support animal welfare during natural disasters by identifying the occupancy status of remote facilities.
- **Resource management for governments:** Supports broader resource management by providing reliable data on facility usage patterns. This can inform decisions about infrastructure development, resource allocation, and regional planning in agricultural zones.

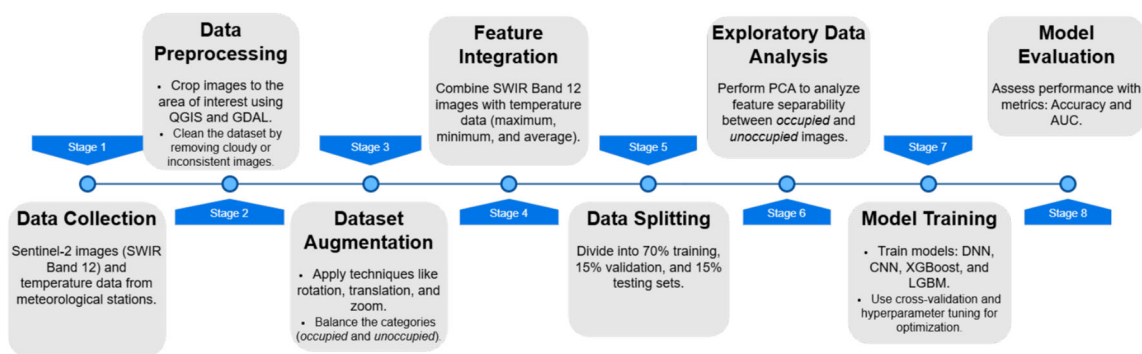


Fig. 1 Methodology Workflow

Materials and methods

The workflow for the machine learning pipeline, depicted in Fig. 1, outlines the sequential steps undertaken in this study to classify farm occupancy using Sentinel-2 satellite data and external temperature information. Given the importance of monitoring agricultural operations, especially in regions with high agricultural productivity, this study focuses on data collected from buildings in four pig farms in Spain in the Ebro Valley.

We have used data from buildings in four pig farms in Spain in the Ebro Valley (municipalities of Albalate, Ballobar, Granen and Tamarite). This is a large geographical region in the northeast of the Iberian Peninsula, identified by the Ebro River basin. It is bounded by the Pyrenees mountain range to the north, the Iberian system to the south and the Catalan Coastal mountain ranges to the east (see). Its climate is continental Mediterranean with wide temperature variations. Winters have temperatures from -1°C to 12°C . Summers are hot and dry, ranging from 18°C to 40°C . This region includes most of the pig production in Spain.

These buildings have been selected as they offer the following features:

- They are located in isolated areas with a minimum of 1000 metres from urban environments (for sanitary reasons). This distance ensures that there is no thermal influence.
- They allocate the animals in a limited space, with a constant temperature when the building is being used. This implies a clear difference in the heat emission according to the occupancy state.
- The buildings are large enough to provide representative data coverage within the 20 m/pixel resolution of Sentinel-2 sensors.
- We have a complete schedule provided by the owners indicating when the buildings are in use and when not.

The information related to these farms consisted of a collection of satellite images covering these farms on different dates, the outdoor temperature at each farm in the image dates, and a report provided by the farm owners of the occupancy of the farms on each date. Specifically, we have downloaded from the Copernicus Open Access Hub² the 72 satellite images available in 2021 from the Sentinel-2 B12 tile T30TYM/EPSC:32630 (see Fig. 2). The Albalate, Ballobar, and Granen farms are correctly visible in these images, but only 65 of them properly show Tamarite due to cloud coverage. Each tile was cropped to select the area covered by the farms. To do this, we have manually generated vector files with the geometry of the farm buildings from orthophotos of the year 2021 using QGIS (see Fig. 3) and use them as template to perform the cropping with GDAL³ (see Fig. 4),

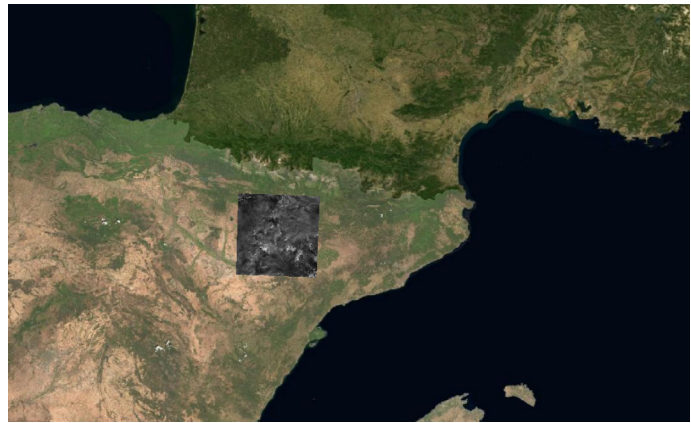
Data processing

This has left us with 281 images ($72 \times 3 + 65$) that were classified into occupied and unoccupied farms using the occupancy data provided by the farm owners. Based on the provided occupancy data, the classification task focuses on determining whether a farm is occupied or unoccupied. Occupied farms correspond to periods when animals are housed in the facilities, while unoccupied farms refer to periods without animal presence. During fattening periods, animals are brought onto the farm, beginning a period of occupancy that ends when the animals are removed. The farmers document these dates, allowing accurate knowledge of when the farms are in use. The result is 206 images with the farms in an occupied state and 75 in an unoccupied one. However, the occupation is not homogeneous in all farms. Albalate has the most images in an occupied state (95.83%), Ballobar (80%), Granen (65%) and Tamarite the least (40.00%). This variability and the limited number of images have forced us to

² <https://scihub.copernicus.eu>, last visit December 2024

³ <https://gdal.org>, last visit October 2024

Fig. 2 Tile used over the reference map



balance the training categories and use data augmentation techniques since some of the used models benefit from it (e.g., convolutional neuronal networks). For the others, they can be seen as neutral, being not relevant or detrimental. Specifically, we have increased the number of images to 3866 and balanced the categories with the following approaches:

- **Rotate the images in a random range of 359°:** It allows some models to learn to recognize objects from multiple orientations, improving its ability to generalize from new images in practical applications.
- **Horizontal/Vertical movement in the image:** Image translation helps some models to improve generalization by introducing variability in the position of objects within the images. This technique simulates actual conditions, making them more robust to perturbations and displacement.
- **Image zoom:** Using images with different zoom levels can help some models recognize and process objects and patterns at various scales, increasing their usefulness and accuracy in real-world applications where objects may appear at different sizes or resolutions.

Regarding the farms analyzed, the external temperature influences the thermal values obtained from the farm buildings, becoming an important factor in the classification process. Specifically, we have employed the maximum, minimum and average temperatures recorded by the nearest weather station on the dates corresponding to the Sentinel-2 images to ensure that the temperature data reflect the local climatic conditions of the farm areas. This information was obtained from the Open Data portal of the Spanish Meteorological Agency (AEMET)⁴. We used the linear distance-based search system provided by that agency. The

distance between each farm and its nearest station varies between 32 and 50 km. Since they are all located in the same climatic zone (delimited by the Ebro Valley), we consider that the precision of the measurements of these stations is adequate for the experiment. Combining these temperature measurements with spectral data from Sentinel-2 provides the basis for analyzing the thermal signals from the farm buildings.

Building on this foundation, the study incorporates data from the Shortwave Infrared (SWIR) Band 12 of Sentinel-2, which operates outside the visible RGB spectrum. While not direct temperature readings, the thermal signals from this band serve as proxies for the spectral responses associated with the conditions of the farm buildings. By integrating these spectral signals with external temperature data, the study ensures robust inputs for the classification models. Finally, the dataset was split into 70% for training, 15% for validation, and 15% for testing, facilitating the evaluation of the model of the performance on unseen data.

In the visual correlation between average temperature and B12 band reflectance (Fig. 5) each farm has a pattern where reflectance values change with temperature variations. This justifies the data fusion strategy used in this study, as these temperature-related spectral variations can indirectly reflect the thermal behaviour of the farm buildings and, thus, the possible human activity inside them. The correlation across the farms demonstrates varying patterns of relationships. These plots show how B12 reflectance varies with changes in average temperature at each studied farm. At some farms, such as 'Albalate' and 'Ballobar,' data points tend to cluster more distinctly or show a pattern that might indicate an underlying relationship between these two variables. While this does not necessarily indicate a strong linear correlation, it suggests that temperature changes may be associated with variations in B12 reflectance. In others, like 'Tamarite,' the dispersion is less clear but still presents a distribution that could be further

⁴ https://www.aemet.es/es/datos_abiertos/AEMET_OpenData, last visit December 2024



Fig. 3 Creation of farm shapefiles



Fig. 4 Pixels selection

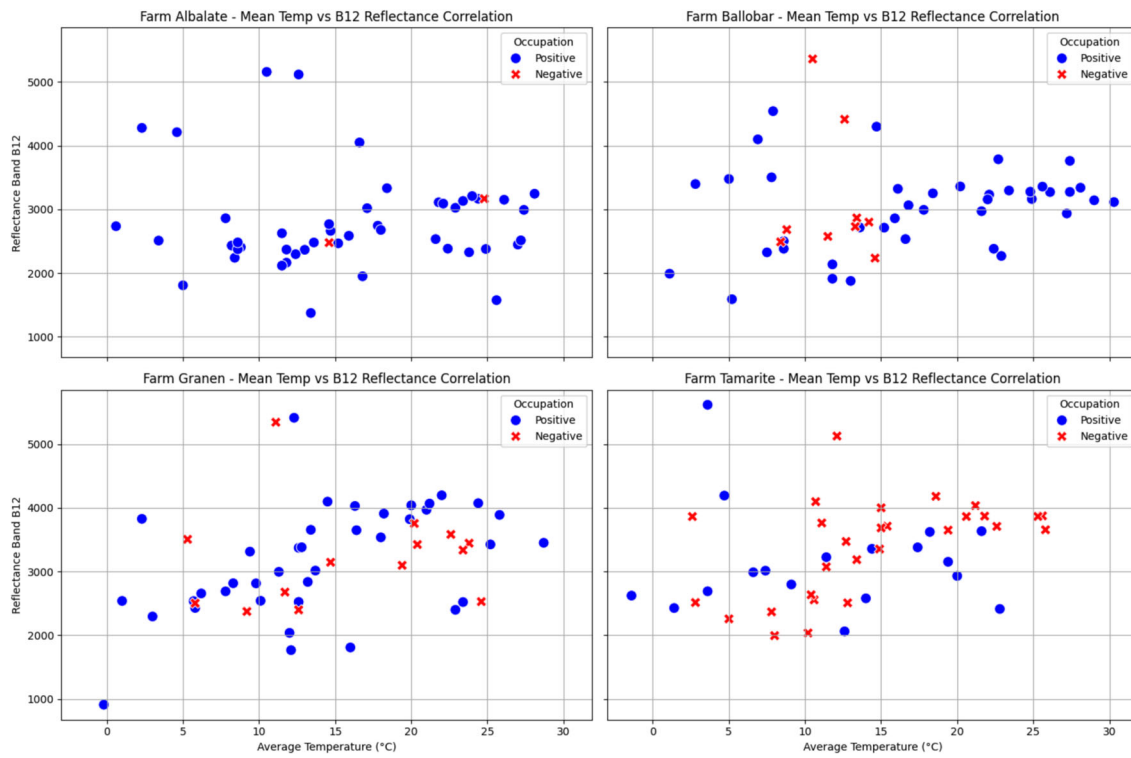


Fig. 5 Correlation between average external temperature and B12 band reflectance in each of the four studied farms

investigated to understand these dynamics better. This visualization supports the notion that fusing temperature data with B12 reflectance is logical and potentially practical. Both variables interact in a way that could be relevant for modelling and predicting phenomena related to environmental conditions and their effects on satellite-detected reflectance. Data fusion allows for a more holistic and detailed understanding of ground conditions, facilitating more robust and potentially more accurate analyses.

Experiments and model descriptions

To evaluate the ability of machine learning models to classify farm occupancy based on remote sensing data, we designed a series of experiments. These experiments leverage diverse input features derived from Sentinel-2 satellite images and complementary external data. By integrating spatial, spectral, and temperature information, we aim to develop robust models capable of accurately predicting occupancy under varying conditions.

The features used as model inputs include:

- **SWIR Band-12 images:** Sentinel-2 data cropped to the area of interest, with a spatial resolution of 20 m/pixel. The image dimensions are 29 rows by 28 columns, representing a pixel resolution 29x28.
- **External temperature data:** Maximum, minimum, and average daily temperatures recorded at nearby weather stations on the corresponding image dates.

Additionally, we have used augmented images generated through rotation, translation, and zoom to increase dataset size and improve model generalization.

To assess the complexity of identifying the use of the buildings in the selected farms, we first applied Principal Component Analysis (PCA) to all features in the dataset to determine whether images depicting occupied buildings can be directly distinguished from those showing vacant buildings. In Fig. 6, we can observe that the data is entirely split by farm, not by occupancy. The data from each farm forms a separate data cluster in which the images with used buildings are mixed with the empty ones. Additionally, each farm behaves thermally differently; therefore, more data from additional buildings in different places and climates will be needed to generalize the results outside the experiment data.

We have performed the following experiments to identify more useful data for detecting human activity from satellite images. In the first analysis, we have aimed to detect human activity using only the original Sentinel-2 images. In a second approach, we have included the exterior temperature (maximum, minimum, and average temperatures of the farm corresponding to the satellite images on the day they were taken). The temperature information is added to the Sentinel-2 images as new pixels in the image, as shown in Fig. 7. The following approach has been to extend the input data used in the second approach using the previously indicated data augmentation techniques to determine if it is helpful for the models that theoretically can take advantage of it to learn more diverse patrons in the images. Finally, we investigated the influence on the prediction of the specific farms in the training data. To do that, we use the input data of the second approach, make four different predictions, each removing one farm from the data, and calculate the average

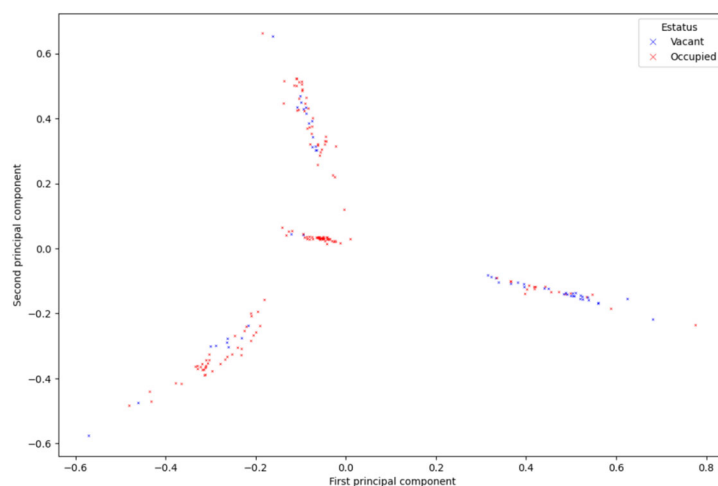


Fig. 6 PCA Analysis of the four agricultural units data

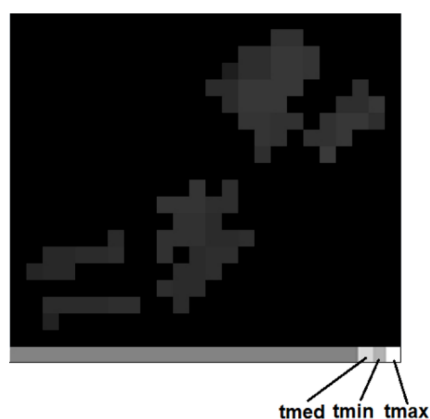


Fig. 7 Integration of temperatures as pixels and channels

of the results. This allows an understanding of how sensitive the performance of the model is to the training data and if the model learns to classify the data or if it only leans to the features of each farm individually.

In this study, we evaluate four models, Dense Neural Networks (DNN), Convolutional Neural Networks CNN, Light Gradient Boosting Machine (LGBM) and eXtreme Gradient Boosting (XGBoost), based on their proven effectiveness in similar remote sensing contexts and their suitability for handling the complexity of Sentinel-2 data, particularly for tasks involving indirect thermal detection. This study's selection of these models is based on theoretical reasoning and empirical evidence derived from recent literature, particularly in applications involving Sentinel-2 data for environmental inference. These models have consistently demonstrated their effectiveness in remote sensing, especially in scenarios involving spectral, complex spatial and temporal patterns. DNNs comprise layers of interconnected nodes capable of modelling non-linear relationships in high-dimensional data. DNNs are especially useful for learning intricate dependencies between spectral bands, such as those needed for indirect thermal inference when working with reflectance in the SWIR range. Previous studies have shown their successful application in vegetation index analysis (Liu et al. 2022; Budi Cahyo Suryo et al. 2019; Saini et al. 2020; Dorffner et al. 2001; Bal and Kayaalp 2021; Tos et al. 2021), soil salinity mapping (Sirpa-Poma et al. 2023), and yield prediction (Aslan et al. 2024). CNN, being multilayer neural networks with convolutional operations, are well-suited for spatial pattern recognition and feature extraction from image data (Chien 2019). Their ability to extract translation-invariant features makes them ideal for applications such as land cover classification (Zhou et al. 2018; Nazari and Yan 2021; Kato et al. 2021), and object detection in heterogeneous environments (Nazari and Yan 2021). In remote

sensing, CNNs are frequently used to analyze Sentinel-2 data for crop type mapping (Wang et al. 2024) and vegetation condition assessment. LGBM is a tree-based model that constructs trees vertically, which improves computational efficiency and scalability in high-dimensional datasets (Ke et al. 2017). LGBM has been successfully applied in remote sensing tasks such as satellite image classification (Bhagwat and Shankar 2019; Jin et al. 2020; Samat et al. 2020; Ha et al. 2021; Tian et al. 2022; Colkesen and Ozturk 2022; Abdikan et al. 2023) and soil salinity modelling (Sirpa-Poma et al. 2023), proving especially effective in structured tabular data derived from spectral indices. XGBoost is another gradient-boosting technique recognized for its robustness and scalability in high-dimensional settings. It builds an ensemble of weak learners (decision trees), optimized iteratively to reduce error (Chen and Guestrin 2016). It has been used effectively in remote sensing for vegetation monitoring, land cover classification, and mineral mapping (Anifadi et al. 2024; Wang et al. 2024). Combining use of these models offers complementary strengths: DNN and CNN provide deep representation learning from raw and spatial data, while XGBoost and LGBM handle feature-based tabular data efficiently. This is particularly useful when working with Sentinel-2 data, where pixel-based (e.g., spatial textures from CNN) and feature-based (e.g., vegetation indices for XGBoost/LGBM) information is available. In this study, their use is further justified by the need to capture subtle patterns associated with indirect thermal activity through the B12 band, a use case not addressed in prior studies (Thomas et al. 2022; Anifadi et al. 2024; Sirpa-Poma et al. 2023; Wang et al. 2024).

The input data is randomly mixed to ensure that the images of occupied and unoccupied farms are randomly separated and do not generate biases. To assess the efficacy of our classification models, We have employed the correlation matrix proposed by Provost and Kohavi (1998) and the associated metrics it provides. The following equations describe the measures used to calculate the quality of the models (Accuracy, Precision, Recall, F1 Score and FPR). In the equations, TP means True Positive, FP means False Positive, FN is False Negative, and TN is True Negative. The accuracy indicates the proportion of correct predictions to the total number of predictions. The precision measures the ability of the model to correctly identify positive cases among all the instances it predicted as positive. The recall evaluates the model's ability to identify all positive cases among all actual positive cases correctly. The F1 Score balances Precision and Recall, which is very useful when there is a mismatch between the classes. Finally, the FPR and TPR show the proportion of negative cases the model incorrectly classified as positive (FPR) and the ratio of positive cases classified as negative

(TPR). Finally, we used the area under the curve (AUC) to quantify class separability. A value of AUC close to 1 indicates that the model can effectively separate classes, while a low value indicates the opposite (Fawcett 2006; Bradley 1997; Hanley and McNeil 1982).

$$\text{Accuracy} = \frac{TP + TN}{TP + TN + FP + FN} \tag{1}$$

$$\text{Recall} = \frac{TP}{TP + FN} \tag{2}$$

$$\text{FPR} = \frac{FP}{FP + TN} \tag{3}$$

$$\text{Precision} = \frac{TP}{TP + FP} \tag{4}$$

$$\text{F1-score} = 2 \cdot \frac{\text{Precision} \cdot \text{Recall}}{\text{Precision} + \text{Recall}} \tag{5}$$

$$\text{TPR} = \frac{TP}{TP + FN} \tag{6}$$

Experimental results

This section describes the results obtained by the previously described models according to the best configurations obtained by a hyperparameter search using OPTUNA (Akiba et al. 2019), an automated hyperparameter framework.

Table 2 shows the performance of each model in all the experiments proposed using the best hyperparameters using Optuna; a Cross-validation was implemented across all models to reduce the risk of overfitting and ensure more generalizable results, using a 70:15:15 ratio for training, testing, and validation.

The results demonstrate that integrating temperature data significantly enhances the detection accuracy across most models. XGBoost is the best model when temperature data is included, achieving a 96% accuracy and a 0.94 Area Under the Curve (AUC). This accuracy is high compared to many classification tasks reported in the provided literature using Sentinel-2 data, such as crop type mapping (often achieving

85-90% with methods like U-Net (Li et al. 2022)), land cover classification (76-96% for specific classes like arable land vs. pastures (Stara and Halounova 2022)), water quality parameter estimation (where R^2 values are often the primary metric, e.g., Chl-a inversion with CNN achieving $R^2 = 0.81$ (Zhu et al. 2024) or turbidity prediction with GBDT achieving $R^2 = 0.88$ (Ma et al. 2021)), or burned area/severity mapping (Kappa often around 0.8-0.9 (Sobrino et al. 2024; Farhadi et al. 2023)). While the direct comparison is complex due to differing tasks and metrics, the 96% accuracy suggests that the inclusion of explicit temperature data makes the detection task relatively separable for the XGBoost model in this specific experimental setup. The consistent high performance of XGBoost aligns with findings in several shared papers where gradient boosting variants (XGBoost, GBDT, LGBM) or Random Forest often yielded top results for various remote sensing prediction and classification tasks (Chen et al. 2023; Liu et al. 2024; Zoratipour et al. 2024; Ma et al. 2021; Li et al. 2025; Yao et al. 2024). Conversely, the DNN showed the relatively lowest performance in most scenarios here.

The substantial boost in accuracy and AUC, when temperature data is added (e.g., XGBoost accuracy jumps from 85% to 96%, CNN from 76% to 88%), underscores the critical value of thermal information for this detection task. This is shown with numerous studies that leverage thermal data or Sentinel-2’s Short-Wave Infrared (SWIR) bands (B11, B12), which are sensitive to temperature and moisture variations. For instance, Land Surface Temperature (LST) retrieval studies explicitly use thermal bands or ML models incorporating atmospheric parameters alongside Sentinel-2 data (Zegaara et al. 2024). Similarly, effective drought monitoring relies on indices combining vegetation state with temperature (e.g., VTCI derived from LST and NDVI) (Li et al. 2025). Active fire detection and severity assessment frequently utilize SWIR bands (B11, B12) or derived indices like NBR, which capture thermal emissions and post-fire effects (Hu et al. 2021; Güler and Kalkan 2022; Rana et al. 2024; Farhadi et al. 2023; Prodromou et al. 2023; Al-hasn and Almuhammad 2022; Sobrino et al. 2024). Furthermore, detecting methane

Table 2 Comparative results in the testing dataset

Model	Images w/o Temp. ^a		Images w/ Temp. ^b		Img. Aug. w/ Temp. ^c		-1 Farm w/ Temp. ^d	
	Accuracy	AUC	Accuracy	AUC	Accuracy	AUC	Accuracy	AUC
DNN	0.78	0.75	0.82	0.80	0.83	0.81	0.76	0.74
CNN	0.76	0.73	0.88	0.86	0.88	0.87	0.76	0.74
XGBoost	0.85	0.88	0.96	0.94	0.83	0.85	0.92	0.90
LGBM	0.81	0.80	0.81	0.80	0.84	0.83	0.81	0.80

^a Images without Temperature.

^b Images with Temperature.

^c Image Augmentation and Temperature.

^d Removing one Farm with Temperature

plumes or gas flaring often involves algorithms sensitive to SWIR bands where methane absorbs or where high temperatures create distinct spectral signatures (Gorroño et al. 2023; Ehret et al. 2022; Kingwill et al. 2022; Turon et al. 2023). The proposed DBB index for dust/biomass burning also leverages SWIR bands (B11, B12) alongside visible bands (Lolli et al. 2024). The effectiveness of the $EOMI_2$ index (using B12 and B4) for detecting manure applications (Marzi et al. 2023) and the importance of SWIR bands in discriminating Fe-Ni laterites from bauxites (Anifadi et al. 2024) further highlight the utility of these spectral regions, likely linked to moisture and mineral composition affecting thermal properties. Therefore, the observed performance gain upon adding temperature data aligns well with the established importance of thermal or SWIR information in related remote sensing applications.

The CNN model demonstrated a significant performance increase with the inclusion of temperature data (Accuracy: 0.76 to 0.88; AUC: 0.73 to 0.86), benefiting slightly more from image augmentation (AUC reaching 0.87). This aligns with CNN's inherent strength in processing image-based spatial and spectral features, as supported by Zhou et al. (2018); Nazari and Yan (2021); Kato et al. (2021). However, it was surpassed by XGBoost here, consistent with findings in some reviewed papers where tree-based ensembles outperformed CNNs for specific tabular/spectral data tasks (Chen et al. 2023; Liu et al. 2024; Ma et al. 2021) (though Zhu et al. (2024) shows CNN superior for Chl-a, contrasting this finding). Other studies also confirm XGBoost's good performance (Bhagwat and Shankar 2019; Jin et al. 2020; Ha et al. 2021; Tos et al. 2021). One possible reason XGBoost outperform CNN is that its decision-tree structure excels on tabular spectral inputs, modelling nonlinear interactions without extensive hyperparameter tuning or large datasets. Its built-in regularization and pruning also make it resilient to missing values, outliers, noise, and minor thermal variations, so it generalizes better in small-sample detection tasks. In contrast, CNNs typically require more detailed data cleaning and more examples to learn subtle pixel-level patterns, causing them to lag on limited-sized spectral datasets. The relative performance can depend highly on the dataset characteristics, feature engineering, and the specific network architecture. The finding that image augmentation provided only marginal benefits, primarily for DNN and LGBM, is noteworthy. This suggests that the augmentation techniques used were not optimal for capturing the features of heat emissions or that the original dataset was sufficiently varied for models like XGBoost and CNN. This tends to appear with the study on soil salinity mapping in Bolivia (Sirpa-Poma et al. 2023), where augmenting a scarce dataset by assigning neighbour pixel values significantly improved Random Forest model accuracy (0.25 to 0.77), demonstrating augmentation's potential in data-limited scenarios. The limited

impact here might imply that the core signal related to temperature is strong enough that artificial data adds little new information or that the augmentation method failed to replicate the heat emission patterns realistically.

The "leave-one-farm-out" experiment provides valuable insight into model generalization. The significant performance drop observed for DNN, CNN, and particularly XGBoost (Accuracy: 96% to 92%; AUC: 0.94 to 0.90) when one farm's data was excluded suggests these models might have learned characteristics specific to the individual farms present in the training set. In contrast, LGBM maintained relatively stable accuracy and AUC (around 0.80-0.83 across scenarios), hinting at potentially better generalization capabilities in this context or perhaps an inability to capture the finer details that led to higher performance for XGBoost when all data was present. Assessing model transferability and robustness across different geographical sites or conditions is a common challenge highlighted in several reviewed papers, such as the difficulties in directly transferring OBIA landslide detection methods in Pakistan (Bacha et al. 2020) or the variable influence of soil texture on SOC prediction across diverse European sites (Wetterlind et al. 2025), which often highlight challenges in generalization. The observed sensitivity to removing one farm highlights the importance of diverse training data and robust validation strategies to ensure model generalization.

This analysis strongly indicates that incorporating temperature data is highly beneficial for the detection task using Sentinel-2 imagery, with XGBoost delivering the best performance (96% accuracy, 0.94 AUC). This aligns with findings across the provided literature emphasizing the importance of thermal information and SWIR bands in diverse environmental monitoring applications. While CNNs also leverage temperature data effectively, tree-based ensembles like XGBoost often prove highly competitive or superior for many remote sensing tasks involving spectral and ancillary data. The limited effect of image augmentation contrasts with its potential benefits in data-scarce situations, as shown elsewhere.

Conclusions and future work

The primary objective of this study was to investigate the feasibility of utilizing Sentinel-2 satellite data to predict the occupancy of isolated buildings in remote areas, aiming to detect activity indoors by correlating heat emissions with external meteorological data, given the limitations of publicly available satellite data and the notable absence of specific sensors capable of detecting direct heat emissions from inside buildings, this research explored whether machine learning models could be trained to interpret the available data effectively. For this task, we evaluated the performance of

four machine learning models (DNN, CNN, XGBoost, and LGBM) using satellite imagery and meteorological information as input data. This approach aligns with the work of Khurana et al. (2023); Song and Lu (2024); Du et al. (2024), who also used Sentinel-2 imagery and neural networks for similar predictive tasks, Khurana et al. (2023) employed multi-temporal imagery and SVM. While Song and Lu (2024) applied ResNet and LSTM networks to model urban landscapes, this demonstrated the effectiveness of neural networks and Du et al. (2024) used CNN and LSTMs, focusing on the importance of integrating additional data, such as meteorology, to improve accuracy.

The experimental findings show the suitability of our proposal; among the evaluated models, XGBoost achieved the best results with an accuracy of 96% and the highest AUC values, indicating its robustness and effectiveness in utilizing additional features such as temperature data. The CNN model significantly improved AUC when incorporating temperature data, suggesting its potential to extract valuable insights from complex input data. The DNN model, while benefiting from data augmentation, indicated a sensitivity to data variability, which could be a consideration for real-world applications where data inconsistency is common. The LGBM model consistent AUC performance across various scenarios suggests its reliability and stability, making it a potentially valuable model for continuous monitoring with varying data inputs; these insights into model performance, particularly the AUC metric, reinforce the potential of integrating meteorological data to enhance predictive accuracy.

The main limitation identified in the research is external. First, the five-day revisit interval of Sentinel-2 satellites may be long for specific applications, making it less suitable for specific scenarios that require more frequent observations; in the same way, other satellites with shorter revisit times usually come with the trade-off of larger pixel sizes, which is not suitable for the precision of the data. Another important challenge is the limited availability of public datasets for training the models, which limits the overall performance and generalizability of the models, the use of Data augmentation has proven to be partially helpful in some tested models. However, these methods are not effective across all cases. The experiment shows that removing one farm reduces XGBoost's accuracy from 96% to 92%, indicating sensitivity to training data. Future work should increase data diversity. As a result, the reliance on publicly accessible satellite imagery generates issues related to the quality and resolution of data, impacting the overall accuracy and applicability of the proposed solutions.

The B12 band has a 20 square meters resolution. This is a limitation that has to be considered when application scenarios are selected. In the experiment, big buildings (more than 1.000 square meters) have been used. Nevertheless, the key point of the detection is to have at least one pixel inside

the building. Depending on the correspondence with the grid of satellite data, the best case would be to have the perfect coincidence between a pixel and a 20-square-meter building. To guarantee at least one pixel with information from the building, it is necessary to have at least around 15×15 meters of buildings (considering the 45° rotation of the building in correspondence with the grid).

As future work to improve the results obtained and reduce the limitations, the authors are exploring ways to combine Sentinel-2 and Sentinel-3 data to enhance image resolution. Additionally, the authors plan to increase the volume of training data and consider additional inputs into the models. Specifically, they aim to reach collaboration agreements with additional farm owners to gather data from their estates, extend the years we consider, and use more information from meteorological data beyond temperature. By pursuing these strategies, the authors hope to develop models that are even more accurate and valuable for stakeholders in the agricultural industry.

One of this study's current limitations is that it relies on a small dataset with specific climatic conditions characteristic of the Mediterranean climate. This climate is defined by well-marked seasons, hot and dry summers, and wet winters, which can influence the environment's spectral response and the accuracy of indirect thermal signal detection. Therefore, extending this methodology to other climatic zones, such as tropical regions, would be particularly valuable, as these areas exhibit distinct atmospheric behaviours, persistent vegetation cover, and high humidity levels.

Applying the approach in tropical climates would help assess its robustness under varying environmental conditions and provide insight into human activity patterns and population dispersion in contexts where many buildings remain unoccupied, unused, or disconnected from service networks. These scenarios pose a challenge for remote sensing of human presence through indirect thermal signals but also represent an opportunity to validate the potential of the Sentinel-2 B12 band under more complex conditions.

It is important to highlight that the data used in this study are private and have been obtained through requests to private sector companies. This collaboration has enabled access to datasets that would otherwise not be available for study. The dependence on externally provided datasets or infrequent ground-truthing campaigns continues to limit the generalizability of the models. Overcoming this limitation will require complementary strategies such as using synthetic data, integrating additional sensors, or developing collaborative networks for real-time information gathering.

Acknowledgements This work has been partially supported by the Aragon Regional Government and the European Union - FEADER (project T59_23R) and the Spanish Government (project PID2020-113353RB-I00). Mario Suaza has been partially supported by the Colombian Ministry of Science, Technology and Innovation (MIN-

CIENCIAS 885/2020). He also wants to thank the Productivity and Competitiveness Research Group from the Universidad del Norte, Colombia for its help in the analysis processes. The authors would also like to thank Luís, Alberto and José María, who provided the occupancy data of the farms used in this paper.

Author Contributions **Mario E. Suaza-Medina:** Formal analysis, Investigation, Validation, Visualization, Roles/Writing - original draft, Writing - review & editing, Data curation.

Javier Lacasta: Conceptualization, Formal analysis, Investigation, Validation, Roles/Writing - original draft, Writing - review & editing, Supervision.

Francisco J. López-Pellicer: Formal analysis, Investigation, Validation, Writing - review & editing.

Rubén Béjar: Formal analysis, Investigation, Validation, Writing - review & editing.

F. Javier Zarazaga-Soria: Conceptualization, Formal analysis, Investigation, Validation, Roles/Writing - original draft, Writing - review & editing, Funding acquisition;

Funding This work has been partially supported by the Aragon Regional Government and the European Union - FEADER (project T59_23R) and the Spanish Government (project PID2020-113353RB-I00). Mario Suaza has been partially supported by the Colombian Ministry of Science, Technology and Innovation (MINCIENCIAS 885/2020).

Data Availability No datasets were generated or analysed during the current study.

Declarations

Conflicts of Interest The authors declare that they have no conflict of interest.

Competing interest The authors declare no competing interests

Ethical Approval This article does not contain any studies with human participants or animals performed by any of the authors.

Open Access This article is licensed under a Creative Commons Attribution 4.0 International License, which permits use, sharing, adaptation, distribution and reproduction in any medium or format, as long as you give appropriate credit to the original author(s) and the source, provide a link to the Creative Commons licence, and indicate if changes were made. The images or other third party material in this article are included in the article's Creative Commons licence, unless indicated otherwise in a credit line to the material. If material is not included in the article's Creative Commons licence and your intended use is not permitted by statutory regulation or exceeds the permitted use, you will need to obtain permission directly from the copyright holder. To view a copy of this licence, visit <http://creativecommons.org/licenses/by/4.0/>.

References

- Abdikan S, Sekertekin A, Narin OG, Delen A, Balik Sanli F (2023) A comparative analysis of slr, mlr, ann, xgboost and cnn for crop height estimation of sunflower using sentinel-1 and sentinel-2. *Adv Space Res* 71(7):3045–3059. <https://doi.org/10.1016/j.asr.2022.11.046>. Recent Advances in Space Research in Monitoring Sustainable Development Goals
- Abdollahi A, Liu Y, Pradhan B, Huete A, Dikshit A, Tran NN (2022) Short-time-series grassland mapping using sentinel-2 imagery and deep learning-based architecture. *Egypt J Remote Sens Space Sci* 25:673–685. <https://doi.org/10.1016/j.ejrs.2022.06.002>
- Akiba T, Sano S, Yanase T, Ohta T, Koyama M (2019) Optuna: A Next-generation Hyperparameter Optimization Framework. *Proceedings of the ACM SIGKDD international conference on knowledge discovery and data mining*, pp 2623–2631
- Alberto Vavassori GG, Brovelli MA (2023) Mapping local climate zones in lausanne (switzerland) with sentinel-2 and prisma imagery: comparison of classification performance using different band combinations and building height data. *Int J Digit Earth* 16(2):4790–4810. <https://doi.org/10.1080/17538947.2023.2283485>
- Al-hasn R, Almuhammad R (2022) Burned area determination using sentinel-2 satellite images and the impact of fire on the availability of soil nutrients in syria. *J Forest Sci* 68:96–106. <https://doi.org/10.17221/122/2021-JFS>
- Alshari EA, Gawali BW (2020) Analysis of machine learning techniques for sentinel-2a satellite images. *J Electr Comput Eng* 2022. <https://doi.org/10.1155/2022/9092299>
- Anifadi A, Sykioti O, Koutroumbas K, Vassilakis E, Vasilatos C, Georgiou E (2024) Discrimination of fe-ni-laterites from bauxites using a novel support vector machines-based methodology on sentinel-2 data. *Remote Sens* 16:2295. <https://doi.org/10.3390/rs16132295>
- Anifadi A, Sykioti O, Koutroumbas K, Vassilakis E, Vasilatos C, Georgiou E (2024) Discrimination of fe-ni-laterites from bauxites using a novel support vector machines-based methodology on sentinel-2 data. *Remote Sens* 16:2295. <https://doi.org/10.3390/rs16132295>
- Aslan MF, Sabanci K, Durdu A, Unlarsen MF (2024) Crop yield prediction using deep learning: A review. *Comput Electron Agri* 212:108318. <https://doi.org/10.1016/j.compag.2024.108318>
- Avila-Zuniga-Nordfeld A, Liwång H, Dalaklis D (2023) In: Johansson TM, Dalaklis D, Fernández JE, Pastra A, Lennan M (eds) Implications of technological innovation and respective regulations to strengthen port and maritime security: An international agenda to reduce illegal drug traffic and countering terrorism at sea, Springer, Cham, pp 135–147. https://doi.org/10.1007/978-3-031-25296-9_7
- Bacha AS, Van Der Werff H, Shafique M, Khan H (2022) Transferability of object-based image analysis approaches for landslide detection in the himalaya mountains of northern pakistan. *Int J Remote Sens* 41:3390–3410. <https://doi.org/10.1080/01431161.2019.1701725>
- Bal F, Kayaalp F (2021) Review of machine learning and deep learning models in agriculture. *Int Adv Res Eng J* 5(2):309–323
- Bhagwat R.U, Shankar U (2019) A Novel Multilabel Classification of Remote Sensing Images Using XGBoost. *IEEE*, ???
- Bradley AE (1997) The evaluation of machine learning algorithms. *Patt Recognit* 30:1145–1159
- Budi Cahyo Suryo PS, Wayan Mustika I, Wahyunggoro O, Wasisto HS (2019) Improved time series prediction using lstm neural network for smart agriculture application. In: 2019 5th international conference on science and technology (ICST), vol 1, pp 1–4. <https://doi.org/10.1109/ICST47872.2019.9166401>
- Chen F, Wang N, Yu B, Wang L (2022) Res2-unet, a new deep architecture for building detection from high spatial resolution images. *IEEE J Select Top Appl Earth Obs Remote Sens* 15:1494–1501. <https://doi.org/10.1109/JSTARS.2022.3146430>
- Chen S, Ogawa Y, Zhao C, Sekimoto Y (2023) Large-scale individual building extraction from open-source satellite imagery via super-resolution-based instance segmentation approach. *ISPRS J Photogramm Remote Sens* 195:129–152. <https://doi.org/10.1016/j.isprs.2022.11.006>
- Chen Y, Dong Y, Wang Y, Zhang F, Liu G, Sun P (2023) Machine learning algorithms for lithological mapping using sentinel-2 and

- srtm dem in highly vegetated areas. *Front Ecol Evol* 11:1250971. <https://doi.org/10.3389/fevo.2023.1250971>
- Chen T, Guestrin C (2016) XGBoost: A scalable tree boosting system. *Proceedings of the ACM SIGKDD international conference on knowledge discovery and data mining* 13-17-Aug:785–794
- Chien JT (2019) *Deep Neural Network*, Academic Press, ???, pp 259–320
- Cho K, Kim Y, Kim Y (2018) Disaggregation of Landsat-8 thermal data using guided SWIR imagery on the scene of wildfire. *Remote Sensing* 10(1). <https://doi.org/10.3390/rs10010105>
- Colkesen I, Ozturk MY (2022) A comparative evaluation of state-of-the-art ensemble learning algorithms for land cover classification using worldview-2, sentinel-2 and rosis imagery. *Arab J Geosci* 15. <https://doi.org/10.1007/s12517-022-10243-x>
- Dhedra R, Paliakkara N, Lobo VB, Gupta D, Sharma V (2021) Smart agri-farming on satellite imageries using machine learning. In: 2021 6th international conference on communication and electronics systems (ICCES), pp 1342–1347. <https://doi.org/10.1109/ICCES51350.2021.9489130>
- Dixit M, Chaurasia K, Mishra VK, Singh D, Lee HN (2022) 6+: A novel approach for building extraction from a medium resolution multi-spectral satellite. *Sustain (Switzerland)* 14. <https://doi.org/10.3390/su14031615>
- Dorffner G, Bischof H, Hornik K (2001) Applying lstm to time series predictable through time-window approaches. *LNCS* 2130:669–676
- dos Santos RS (2020) Estimating spatio-temporal air temperature in london (uk) using machine learning and earth observation satellite data. *Int J Appl Earth Obs Geoinf* 88. <https://doi.org/10.1016/j.jag.2020.102066>
- Du S, Zheng M, Guo L, Wu Y, Li Z, Liu P (2024) Urban building function classification based on multisource geospatial data: a two-stage method combining unsupervised and supervised algorithms. *Earth Sci Inf* 17:1179–1201. <https://doi.org/10.1007/s12145-024-01250-5>
- Ehret T, De Truchis A, Mazzolini M, Morel JM, Facciolo G (2022) Automatic methane plume quantification using sentinel-2 time series. In: 2022 IEEE (IGARSS), pp 3024–3027. <https://doi.org/10.1109/IGARSS46834.2022.9884134>
- Farhadi H, Ebadi H, Kiani A (2023) Badi: A novel burned area detection index for sentinel-2 imagery using google earth engine platform. In: *ISPRS annals of the photogrammetry, remote sensing and spatial information sciences*, vol X-4/W1-2022, pp 179–186. <https://doi.org/10.5194/isprs-annals-X-4-W1-2022-179-2023>
- Fawcett T (2006) An introduction to roc analysis. *Pattern Recognit Lett* 27:861–874. <https://doi.org/10.1016/j.patrec.2005.10.010>
- Froehlich A, Taiatu CM (2020) *Practical Use of Satellite Data in Support of Human Rights*, Springer, Cham, pp 49–124. https://doi.org/10.1007/978-3-030-35426-8_2
- Garzón J, Molina I, Velasco J, Calabia A (2021) A remote sensing approach for surface urban heat island modeling in a tropical colombian city using regression analysis and machine learning algorithms. *Remote Sens* 13. <https://doi.org/10.3390/rs13214256>
- Ge X, Ding J, Teng D, Wang J, Huo T, Jin X, Wang J, He B, Han L (2022) Updated soil salinity with fine spatial resolution and high accuracy: The synergy of sentinel-2 msi, environmental covariates and hybrid machine learning approaches. *Catena* 212:106054. <https://doi.org/10.1016/j.catena.2022.106054>
- Gorroño J, Varon DJ, Irakulis-Loitxate I, Guanter L (2023) Understanding the potential of sentinel-2 for monitoring methane point emissions. *Atmos Meas Tech* 16:89–107. <https://doi.org/10.5194/amt-16-89-2023>
- Güler m, Kalkan K () Sentinel-3 verileri ile aktif yangın tespiti ve sentinel-2 verileri ile doğrulanması (detection of active fires with sentinel-3 data and their verification through the use of sentinel-2 data). *Turk J Remote Sens GIS* 3:86–97. <https://doi.org/10.48123/rsgis.1095460>
- Ha NT, Manley-Harris M, Pham TD, Hawes I (2021) The use of radar and optical satellite imagery combined with advanced machine learning and metaheuristic optimization techniques to detect and quantify above ground biomass of intertidal seagrass in a new zealand estuary. *Int J Remote Sens* 42(12):4712–4738. <https://doi.org/10.1080/01431161.2021.1899335>
- Hanley JA, McNeil BJ (1982) The meaning and use of the area under a receiver operating characteristic (roc) curve. *Radiology* 143(1):29–36
- Hrisko J, Ramamurthy P, Gonzalez JE (2021) Estimating heat storage in urban areas using multispectral satellite data and machine learning. *Remote Sens Environ* 252:112125. <https://doi.org/10.1016/j.rse.2020.112125>
- Hu X, Ban Y, Nascetti A (2021) Sentinel-2 msi data for active fire detection in major fire-prone biomes: A multi-criteria approach. *Int J Appl Earth Obs Geoinf* 101:102347. <https://doi.org/10.1016/j.jag.2021.102347>
- Jin Q, Fan X, Liu J, Xue Z, Jian H (2020) Estimating tropical cyclone intensity in the south china sea using the xgboost model and fengyun satellite images. *Atmos* 11(4). <https://doi.org/10.3390/atmos11040423>
- Kafy AA, Faisal AA, Shuvo RM, Naim MNH, Sikdar MS, Chowdhury RR, Islam MA, Sarker MHS, Khan MHH, Kona MA (2021) Remote sensing approach to simulate the land use/land cover and seasonal land surface temperature change using machine learning algorithms in a fastest-growing megacity of bangladesh. *Remote Sens Appl Soc Environ* 21:100463. <https://doi.org/10.1016/j.rsase.2020.100463>
- Kato S, Miyamoto H, Amici S, Oda A, Matsushita H, Nakamura R (2021) Automated classification of heat sources detected using SWIR remote sensing. *Int J Appl Earth Obs Geoinf* 103(April):102491
- Ke G, Meng Q, Finley T, Wang T, Chen W, Ma W, Ye Q, Liu TY (2017) LightGBM: A highly efficient gradient boosting decision tree. *Adv Neural Inf Process Syst* 2017-Decem(Nips):3147–3155
- Khurana Y, Soni PK, Bhatt DP (2023) Svm-based classification of multi-temporal sentinel-2 imagery of dense urban land cover of delhincr region. *Earth Sci Inf* 16:1765–1777. <https://doi.org/10.1007/s12145-023-01008-5>
- Kim YW, Kim TH, Shin J, Lee DS, Park YS, Kim Y, Cha YK (2022) Validity evaluation of a machine-learning model for chlorophyll a retrieval using sentinel-2 from inland and coastal waters. *Ecol Indic* 137:108737. <https://doi.org/10.1016/j.ecolind.2022.108737>
- Kingwill W, Huppertz R, Kumar S, Mouton R, Adamczyk W, Sherwin E (2022) Guided transformer network for detecting methane emissions in sentinel-2 satellite imagery. *arXiv preprint (NA)*. Preprint/Submitted
- Li G, Cui J, Han W, Zhang H, Huang S, Chen H, Ao J (2022) Crop type mapping using time-series sentinel-2 imagery and u-net in early growth periods in the hetao irrigation district in china. *Comput Electron Agri* 203:107478. <https://doi.org/10.1016/j.compag.2022.107478>
- Li M, Wang P, Tansey K, Sun Y, Guo F, Zhou J (2025) Improved field-scale drought monitoring using modis and sentinel-2 data for vegetation temperature condition index generation through a fusion framework. *Comput Electron Agri* 234:110256. <https://doi.org/10.1016/j.compag.2024.110256>
- Liu S, Zhang J, Li J, Li Y, Zhang J, Wu X (2021) Simulating and mitigating extreme urban heat island effects in a factory area based on machine learning. *Build Environ* 202:108051. <https://doi.org/10.1016/j.buildenv.2021.108051>
- Liu ZYC, Chamberlin AJ, Tallam K, Jones IJ, Lamore LL, Bauer J, Bresciani M, Wolfe CM, Casagrandi R, Mari L, Gatto M, Diongue AK, Toure L, Rohr JR, Riveau G, Jouanard N, Wood CL, Sokolow

- SH, Mandle L, Daily G, Lambin EF, Leo GAD (2022) Deep learning segmentation of satellite imagery identifies aquatic vegetation associated with snail intermediate hosts of schistosomiasis in senegal, africa. *Remote Sens* 14. <https://doi.org/10.3390/rs14061345>
- Liu P, Ren C, Yang X, Wang Z, Jia M, Zhao C, Yu W, Ren H (2024) Combining sentinel-2 and diverse environmental data largely improved aboveground biomass estimation in china's boreal forests. *Sci Rep* 14:27528. <https://doi.org/10.1038/s41598-024-78615-9>
- Lolli S, Alparone L, Arienzo A, Garzelli A (2024) Characterizing dust and biomass burning events from sentinel-2 imagery. *Atmos* 15:672. <https://doi.org/10.3390/atmos15060672>
- Lyu F, Wang S, Han SY, Catlett C, Wang S (2022) An integrated cyberGIS and machine learning framework for fine-scale prediction of urban heat island using satellite remote sensing and urban sensor network data. *Urban Inf* 1(1):6
- Ma Y, Song K, Wen Z, Liu G, Shang Y, Lyu L, Du J, Yang Q, Li S, Tao H, Hou J (2021) Remote sensing of turbidity for lakes in northeast china using sentinel-2 images with machine learning algorithms. *IEEE J Select Top Appl Earth Obs Remote Sens* 14:9132–9146. <https://doi.org/10.1109/JSTARS.2021.3110421>
- Marchese F, Genzano N, Neri M, Falconieri A, Mazzeo G, Pergola N (2019) A multi-channel algorithm for mapping volcanic thermal anomalies by means of sentinel-2 msi and landsat-8 oli data. *Remote Sens* 11. <https://doi.org/10.3390/rs11232876>
- Marzi D, Dell'Acqua F, Trichakis I (2023) Assessing compliance to eu nitrate pollution regulations by detecting manure applications in time series of sentinel-2 acquisitions. In: 2023 IEEE (IGARSS), pp 2103–2106. <https://doi.org/10.1109/IGARSS52108.2023.10282617>
- Memduhoğlu A, Fulman N, Zipf A (2024) Enriching building function classification using large language model embeddings of openstreetmap tags. *Earth Sci Inf*. <https://doi.org/10.1007/s12145-024-01463-8>
- Munyati C (2024) Relating urban land surface temperature to vegetation leafing using thermal imagery and vegetation indices. *Earth Sci Inf*. <https://doi.org/10.1007/s12145-024-01443-y>
- Natale LD, Svetozarevic B, Heer P, Jones CN (2023) Towards scalable physically consistent neural networks: An application to data-driven multi-zone thermal building models. *Appl Energy* 340. <https://doi.org/10.1016/j.apenergy.2023.121071>
- Nazari F, Yan W (2021) Convolutional versus dense neural networks: Comparing the two neural networks performance in predicting building operational energy use based on the building shape. *CoRR arXiv:2108.12929*
- Nurkarim W, Wijayanto AW (2023) Building footprint extraction and counting on very high-resolution satellite imagery using object detection deep learning framework. *Earth Sci Inf* 16:515–532. <https://doi.org/10.1007/s12145-022-00895-4>
- Pati C, Panda AK, Tripathy AK, Pradhan SK, Patnaik S (2020) A novel hybrid machine learning approach for change detection in remote sensing images. *Eng Sci Technol Int J* 23(5):973–981. <https://doi.org/10.1016/j.jestech.2020.01.002>
- Paul A, Bhoumik S (2022) Classification of hyperspectral imagery using spectrally partitioned hyperunet. *Neural Comput Appl* 34:2073–2082. <https://doi.org/10.1007/s00521-021-06532-3>
- Prodromou M, Cerra D, Themistocleous K, Schreier G, Krauss T, Hadjimitsis D (2023) The importance of earth observation for monitoring cultural heritage sites affected by fire events: The case study of arakapas, cyprus using sentinel 2 data. In: The international archives of the photogrammetry, remote sensing and spatial information sciences, vol XLVIII-M-1-2023, pp 263–269. <https://doi.org/10.5194/isprs-archives-XLVIII-M-1-2023-263-2023>
- Provost F, Kohavi R (1998) Glossary of terms. *J. Mach Learn* 30(2–3):271–274
- Rahman A, Abdullah HM, Tanzir MT, Hossain MJ, Khan BM, Miah MG, Islam I (2020) Performance of different machine learning algorithms on satellite image classification in rural and urban setup. *Remote Sens Appl Soc Environ* 20:100410. <https://doi.org/10.1016/j.rsase.2020.100410>
- Rana RS, Vidyarthi A, Prakash R, Dubey VP (2024) Development of algorithm for detection of forest fire in himalayan region using sentinel – 2 msi images. In: 2024 15th international conference on computing communication and networking technologies (ICC-CNT). <https://doi.org/10.1109/ICCNT61001.2024.10724679>
- Saini U, Kumar R, Jain V, Krishnajith MU (2020) Univariate time series forecasting of agriculture load by using lstm and gru mms. In: 2020 IEEE students conference on engineering & systems (SCES), pp 1–6. <https://doi.org/10.1109/SCES50439.2020.9236695>
- Samat A, Li E, Wang W, Liu S, Lin C, Abuduwaili J (2020) Meta-xgboost for hyperspectral image classification using extended mser-guided morphological profiles. *Remote Sens* 12(12). <https://doi.org/10.3390/rs12121973>
- Sarrica F (2022) The use of human trafficking detection data for modelling static and dynamic determinants of human trafficking flows. *Eur J Crim Policy Res* 28(4):483–501. <https://doi.org/10.1007/s10610-020-09460-5>
- Sirpa-Poma JW, Satge F, Resongles E, Pillco-Zolá R, Molina-Carpio J, Flores Colque MG, Ormachea M, Pacheco Mollinedo P, Bonnet MP (2023) Towards the improvement of soil salinity mapping in a data-scarce context using sentinel-2 images in machine-learning models. *Sensors* 23:9328. <https://doi.org/10.3390/s23239328>
- Sobrinho JA, Llorens R, Fernández C, Fernández-Alonso JM, Vega JA (2024) Methodology for burned areas delimitation and fire severity assessment using sentinel-2 data. A case study of forest fires occurred in spain between 2018 and 2023. *Recent Adv Remote Sens* 2:240002. <https://doi.org/10.62880/rars.240002>
- Song T, Lu G (2024) Urban landscape modeling and algorithms under machine learning and remote sensing data. *Earth Sci Inf* 17:2303–2316. <https://doi.org/10.1007/s12145-024-01293-8>
- Stara L, Halounova L () Classification of selected corine classes using sentinel-2 data. In: The international archives of the photogrammetry, remote sensing and spatial information sciences, vol XLIII-B3-2022, pp 175–180. <https://doi.org/10.5194/isprs-archives-XLIII-B3-2022-175-2022>
- Suaza-Medina ME, Laguna J, Béjar R, Zarazaga-Soria FJ, Lacasta J (2024) Evaluating the efficiency of ndvi and climatic data in maize harvest prediction using machine learning. *Int J Digit Earth* 17(1):2359565. <https://doi.org/10.1080/17538947.2024.2359565>
- Talukdar S, Singha P, Mahato S, Shahfahad, Pal S, Liou YA, Rahman A (2020) Land-use land-cover classification by machine learning classifiers for satellite observations—a review. *Remote Sens* 12 (7). <https://doi.org/10.3390/rs12071135>
- Tellman B, Magliocca NR, Turner BL, Verburg PH (2020) Understanding the role of illicit transactions in land-change dynamics. *Nat Sustain* 3(3):175–181. <https://doi.org/10.1038/s41893-019-0457-1>
- The-European-Space-Agency (2015) Sentinel-2, MultiSpectral Instrument (MSI) Overview. <https://sentinels.copernicus.eu/web/sentinel/technical-guides/sentinel-2-msi/msi-instrument> Accessed 05 Dec 2022
- Thomas A, Radzuma T, Mukosi NC (2022) Usefulness of sentinel-2 satellite data to aid in geoscientific mapping work: a case study of giyani greenstone belt area. *Episodes* 45:38–51. <https://doi.org/10.18814/epiiugs/2022/022038>
- Tian S, Guo H, Xu W, Zhu X, Wang B, Zeng Q, Mai Y, Huang JJ (2022) Remote sensing retrieval of inland water quality parameters using sentinel-2 and multiple machine learning algorithms. *Environ Sci Poll Res*. <https://doi.org/10.1007/s11356-022-23431-9>
- Tos H, Mendes GS, Cordeiro D, Grosso N, Costa H, Benevides P, Caetano M (2021) Evaluation of xgboost and lgbm performance in tree species classification with sentinel-2 data. In: 2021 IEEE

- IGARSS, pp 5803–5806. <https://doi.org/10.1109/IGARSS47720.2021.9553031>
- Turon L, Blanco B, Darynova Z, Killisly C, Dubucq D, Arnould N (2023) Quantifying flaring from space on multispectral images calibrated with in-situ flowmeters. In: 2023 IEEE (IGARSS), pp 2770–2773. <https://doi.org/10.1109/IGARSS52108.2023.10282781>
- Vasilakos C, Kavroudakis D, Georganta A (2020) Machine learning classification ensemble of multitemporal sentinel-2 images: The case of a mixed mediterranean ecosystem. *Remote Sens* 12. <https://doi.org/10.3390/rs12122005>
- Wahbi M, El Bakali I, Ez-zahouani B, Azmi R, Moujahid A, Zouiten M, Alaoui OY, Boulaassal H, Maatouk M, El Kharki O (2023) A deep learning classification approach using high spatial satellite images for detection of built-up areas in rural zones: Case study of souss-massa region - morocco. *Remote Sens Appl Soc Environ* 29:100898. <https://doi.org/10.1016/j.rsase.2022.100898>
- Wang Y, Hu X (2022) Machine learning-based image recognition for rural architectural planning and design. *Neural Comput Appl*. <https://doi.org/10.1007/s00521-022-07799-w>
- Wang Y, Wang H, Wang C, Zhang S, Wang R, Wang S, Duan J (2024) Co-kriging-guided interpolation for mapping forest aboveground biomass by integrating global ecosystem dynamics investigation and sentinel-2 data. *Remote Sens* 16:2913. <https://doi.org/10.3390/rs16162913>
- Wetterlind J, Simmler M, Castaldi F, Boruvka L, Gabriel JL, Gomes LC, Khosravi V, Kıvrak C, Koparan MH, Lázaro-López A, Łopatka A, Liebisch F, Rodriguez JA, Savaş A, Stenberg B, Tunçay T, Vinci I, Volungevicius J, Zydelis R, Vaudour E (2025) Influence of soil texture on the estimation of soil organic carbon from sentinel-2 temporal mosaics at 34 european sites. *Eur J Soil Sci*. <https://doi.org/10.1111/ejss.13565>
- Yan S, Yao X, Zhu D, Liu D, Zhang L, Yu G, Gao B, Yang J, Yun W (2021) Large-scale crop mapping from multi-source optical satellite imageries using machine learning with discrete grids. *Int J Appl Earth Obs Geoinf* 103. <https://doi.org/10.1016/j.jag.2021.102485>
- Yao S, Tan K, Wang Y, Zhang W, Liu S, Yang J (2024) Estimating terrain elevations at 10 m resolution by integrating random forest machine learning model and icesat-2, sentinel-1, and sentinel-2 satellite remotely sensed data. *Int J Appl Earth Obs Geoinf* 132:104010. <https://doi.org/10.1016/j.jag.2024.104010>
- Zegaara A, Telli A, Ounoki S, Shahabi H, Rueda F (2024) Data-driven approach for land surface temperature retrieval with machine learning and sentinel-2 data. *Remote Sens Appl Soc Environ* 36:101357. <https://doi.org/10.1016/j.rsase.2024.101357>
- Zhang T, Su J, Xu Z, Luo Y, Li J (2021) Sentinel-2 satellite imagery for urban land cover classification by optimized random forest classifier. *Applied Sciences (Switzerland)* 11:1–17. <https://doi.org/10.3390/app11020543>
- Zhou Z, Li S, Shao Y (2018) Crops classification from sentinel-2a multi-spectral remote sensing images based on convolutional neural networks. (IGARSS) 2018-July, 5300–5303. <https://doi.org/10.1109/IGARSS.2018.8518860>
- Zhu W, Liu S, Luan K, Xu Y, Liu Z, Cao T, Wang P (2024) Research on the inversion of chlorophyll-a concentration in the hong kong coastal area based on convolutional neural networks. *J Marine Sci Eng* 12:1119. <https://doi.org/10.3390/jmse12071119>
- Zoratipour E, Heidari Motlagh A, Soltani Mohammadi A (2024) Monitoring nitrogen and leaf sheath moisture in sugarcane fields using satellite images and artificial intelligence (case study: Amir kabir agro industrial). *Iran J Irrig Water Eng* 15:36–54. <https://doi.org/10.22125/iwe.2024.482662.1835>

Publisher's Note Springer Nature remains neutral with regard to jurisdictional claims in published maps and institutional affiliations.